



MIT Open Access Articles

A Blood-Resistant Surgical Glue for Minimally Invasive Repair of Vessels and Heart Defects

The MIT Faculty has made this article openly available. **Please share** how this access benefits you. Your story matters.

Citation	Lang, N., et al. "A Blood-Resistant Surgical Glue for Minimally Invasive Repair of Vessels and Heart Defects." <i>Science Translational Medicine</i> 6 218 (2014).
As Published	10.1126/SCITRANSLMED.3006557
Publisher	American Association for the Advancement of Science (AAAS)
Version	Author's final manuscript
Citable link	https://hdl.handle.net/1721.1/134265
Terms of Use	Creative Commons Attribution-Noncommercial-Share Alike
Detailed Terms	http://creativecommons.org/licenses/by-nc-sa/4.0/



Published in final edited form as:

Sci Transl Med. 2014 January 8; 6(218): 218ra6. doi:10.1126/scitranslmed.3006557.

A Blood-Resistant Surgical Glue for Minimally Invasive Repair of Vessels and Heart Defects

Nora Lang^{1,*†}, Maria J. Pereira^{2,3,*}, Yuhan Lee^{2,‡}, Ingeborg Friehs^{1,‡}, Nikolay V. Vasilyev¹, Eric N. Feins¹, Klemens Ablasser¹, Eoin D. O'Ceirbhail^{2,§}, Chenjie Xu^{2,||}, Assunta Fabozzo¹, Robert Padera⁴, Steve Wasserman⁵, Franz Freudenthal⁶, Lino S. Ferreira³, Robert Langer⁷, Jeffrey M. Karp², and Pedro J. del Nido¹

Jeffrey M. Karp: jmkarp@partners.org; Pedro J. del Nido: pedro.delnido@cardio.chboston.org

¹Department of Cardiac Surgery, Boston Children's Hospital, Harvard Medical School, 300 Longwood Avenue, Boston, MA 02115, USA

²Division of Biomedical Engineering, Department of Medicine, Center for Regenerative Therapeutics, Brigham and Women's Hospital, Harvard Medical School, Harvard Stem Cell Institute, Harvard-MIT Division of Health Sciences and Technology, 65 Landsdowne Street, Cambridge, MA 02139, USA

³Biotechnology Innovation Center and Center of Neurosciences and Cell Biology, University of Coimbra, 3004-517 Coimbra, Portugal

⁴Department of Pathology, Brigham and Women's Hospital, 75 Francis Street, Boston, MA 02115, USA

⁵Department of Biological Engineering, Massachusetts Institute of Technology, 500 Main Street, Cambridge, MA 02139, USA

⁶Department of Pediatric Cardiology, Kardiozentrum, Obrajés, Calle 14, 669 La Paz, Bolivia

⁷Department of Chemical Engineering and the David H. Koch Institute for Integrative Cancer Research, Massachusetts Institute of Technology, Cambridge, MA 02139, USA

Correspondence to: Jeffrey M. Karp, jmkarp@partners.org; Pedro J. del Nido, pedro.delnido@cardio.chboston.org.

*These authors are first co-authors.

†Present address: Department of Congenital Heart Defects and Pediatric Cardiology, Heart Center Freiburg, Mathildenstrasse 1, 79106 Freiburg, Germany.

‡These authors are second co-authors.

§Present address: School of Mechanical & Materials Engineering, University College Dublin, Dublin 4, Ireland.

||Present address: Division of Bioengineering, Department of Chemical and Biomedical Engineering, Nanyang Technological University, Singapore 637457, Singapore.

Author contributions: N.L., M.J.P., R.L., J.M.K., and P.J.d.N. developed the concept and designed the experiments. N.L., M.J.P., Y.L., and C.X. performed the adhesion tests. N.L., M.J.P., I.F., N.V.V., E.N.F., K.A., and A.F. performed the in vivo experiments. M.J.P. and Y.L. performed the synthesis and chemical characterization of the materials. N.L., M.J.P., I.F., E.D.O., S.W., and F.F. designed and characterized the devices for patch application. N.L. performed the echocardiography and analyzed the images. N.L., M.J.P., J.M.K., L.S.F., Y.L., and P.J.d.N. analyzed the data. N.L. and M.J.P. performed the statistical analysis. R.P. performed the histological analysis of tissue samples. N.L., M.J.P., J.M.K., and P.J.d.N. wrote the manuscript. All authors provided critical feedback on the manuscript.

Competing interests: J.M.K. and R.L. hold equity in Gecko Biomedical, a company that has an option to license IP generated by J.M.K. and R.L. and that may benefit financially if the IP is licensed and further validated. The interests of J.M.K. and R.L. were reviewed and are subject to a management plan overseen by their institutions in accordance with their conflict of interest policies. J.M.K., R.L., P.J.d.N., L.S.F., N.L., and M.J.P. have filed patents based on materials described in this manuscript.

Abstract

Currently, there are no clinically approved surgical glues that are nontoxic, bind strongly to tissue, and work well within wet and highly dynamic environments within the body. This is especially relevant to minimally invasive surgery that is increasingly performed to reduce postoperative complications, recovery times, and patient discomfort. We describe the engineering of a bioinspired elastic and biocompatible hydrophobic light-activated adhesive (HLAA) that achieves a strong level of adhesion to wet tissue and is not compromised by preexposure to blood. The HLAA provided an on-demand hemostatic seal, within seconds of light application, when applied to high-pressure large blood vessels and cardiac wall defects in pigs. HLAA-coated patches attached to the interventricular septum in a beating porcine heart and resisted supraphysiologic pressures by remaining attached for 24 hours, which is relevant to intracardiac interventions in humans. The HLAA could be used for many cardiovascular and surgical applications, with immediate application in repair of vascular defects and surgical hemostasis.

Introduction

Technologies for sealing or attaching devices to tissues without tissue penetration or compression exhibit major limitations, and this has been a barrier for the development of less invasive procedures. Sutures can be technically challenging and time-consuming, especially within a minimally invasive procedure (MIP); can cause local tissue damage; and do not provide an immediate waterproof seal. Existing tissue adhesives have been associated with poor control over adhesion activation, limited adhesion strength, or toxicity (1, 2).

Minimally invasive reconstructive cardiovascular surgery is being pursued to avoid complications from invasive open-heart procedures and cardiopulmonary bypass (CPB); however, one of the main challenges is the inability to reconnect tissue or attach prosthetic materials in a dynamic environment, such as continuous tissue contractions and blood flow, and in the presence of blood. Furthermore, despite their routine use, sutures and staples are associated with tissue damage caused by deep piercing and ischemia (3). This becomes critical when addressing friable tissue (for example, after myocardial infarction or in young infants) or structures near specialized tissue, which ensures the function of specific organs (for example, heart conduction system) (4–7).

Current clinically available adhesives, such as medical-grade cyanoacrylate (CA) or fibrin sealant, can be easily washed out under *in vivo* dynamic conditions and either are toxic or exhibit weak adhesive properties such that they cannot withstand the forces inside the cardiac chambers and major blood vessels (8, 9). Also, many of these adhesives exhibit “activation” properties that make fine adjustments or repositioning of the devices very difficult. Moreover, many adhesives under development achieve tissue adhesion through chemical reaction with functional groups at the tissue surface, and thus become ineffective in the presence of blood (10).

We aimed to develop a stable glue precursor that could be applied to wet substrates, without activation or displacement. We were inspired by the insect footpad as well as the viscous secretions from slugs and sand-castle worms that include water-immiscible components that

are not easily washed out in aqueous environments; these fluids can thus create stable adhesive bonds underwater (11–13). These secretions also displace water and fill gaps on the substrate to maximize transient adhesion via increased contact area and frictional and viscous forces (12). Synthetic hydrophobic adhesives have been recently developed (12,14), including coacervates inspired by sandcastle worm glue that offer practical advantages within wet environments. Towards an approach that addressed key design criteria for cardiovascular applications, we envisioned the use of a biomimetic, stable, water-insoluble precursor that could resist washout *in vivo*, be cured *in situ* via light activation, and achieve a water-tight but flexible bond.

Although light-activated adhesives have been described previously (15-19), most of these adhesives were hydrophilic, leading to substantial swelling and quick washout in the presence of shear stress (20). Thus, we turned to a biocompatible and biodegradable hydrophobic prepolymer, poly(glycerol sebacate acrylate) (PGSA), that could be cross-linked using ultraviolet (UV) light. PGSA is composed of two naturally occurring monomers: glycerol, a basic building block of lipids, and sebacic acid, a metabolic intermediate of fatty acids. Both glycerol and sebacic acid exist in U.S. Food and Drug Administration (21). We hypothesized that by modulating material properties and curing conditions, we could engineer the material to achieve substantial adhesion with soft tissues.

Here, we show that a prepolymer of PGSA mixed with a photoinitiator, comprising the UV cross-linkable hydrophobic light-activated adhesive (HLAA), was not easily washed out from a tissue surface and retained its adhesive strength during prolonged contact with blood. Once activated, the HLAA provided stronger adhesion than standard sealants such as fibrin, even in a highly dynamic environment. We engineered this soft and elastic material for maximal adhesion and demonstrated its effectiveness for the closure of challenging cardiovascular defects in both small and large animal models. The large animals used here replicate human surgical procedures commonly performed, such as repair of blood vessel lacerations or closure of wall defects within the heart.

Results

Engineered HLAA tissue adhesion

Before curing, the HLAA was a highly viscous, water-immiscible prepolymer that could be spread easily over a surface (Fig. 1A). Rheological characterization confirmed the viscous behavior of the material (fig. S1A). Minimal changes in viscosity were observed for different shear rates: a viscosity change from 15.4 ± 0.8 Pa·s to 9.8 ± 1.4 Pa·s (fig. S1B). Upon exposure to UV light in the presence of a photoinitiator, cross-linking occurred and the HLAA became a flexible polymeric film (Fig. 1, A and B).

Initially, multiple compositions of the HLAA were evaluated to maximize adhesive strength under wet conditions. A controlled test apparatus was established to assure consistent compression of the HLAA-coated patch against cardiac tissue during curing (Fig. 1C). We found that 0.5 mol of acrylate groups per 1 mol of glycerol molecule in the prepolymer, as determined through nuclear magnetic resonance (NMR) imaging, provided the strongest adhesion to cardiac tissue (fig. S2). A low degree of acrylation resulted in cohesive failure of

the material at lower forces owing to its limited cross-linking. For a degree of acrylation of 0.5 mol/mol glycerol, the polymeric networks generated were elastic and could be cyclically compressed for at least 100 cycles (Fig. 1B), with minimal changes in the compression modulus of the material. The cured HLAA had a compression modulus of 3.8 ± 0.8 MPa ($n = 4$) during the first cycle of compression. The modulus increased to 4.2 ± 0.6 MPa for the second compression and remained relatively constant for subsequent cycles (Fig. 1B).

The capacity of the HLAA to secure prosthetic patch materials was evaluated through pull-off adhesion testing (Fig. 1C). Poly(glycerol sebacate urethane) (PGSU) (22) was selected as patch material given its superior UV light transparency (fig. S3). Curing times, light intensities, and preload during the curing process were varied to determine optimal conditions for maximal adhesive strength. The HLAA reached its maximum adhesion force after 5 s of UV light exposure, when using a light intensity of 0.38 W/cm² (Fig. 1D). For these curing conditions, the HLAA had about 50% of the adhesive strength of CA and was about 275% stronger than a commercially available fibrin sealant (Fig. 1D). In addition, no significant differences were found between the *in vivo* adhesive strength of CA- and HLAA-coated patches after 2 days of attachment to the epicardium in a rat model (Fig. 1E).

The HLAA networks were evaluated through Fourier transform infrared (FTIR) before and after 5 s of UV curing. The intensity of the peak at 1635 cm⁻¹, corresponding to the absorption of acrylate groups, decreased upon exposure to UV light (fig. S4), indicating polymer cross-linking. Upon variation of the light intensity, no major difference in adhesive strength was observed (fig. S5A). Thus, a light intensity of 0.38 W/cm² was selected for the remainder of this study. Increasing preload correlated with an increase in adhesive strength (fig. S5B), likely owing to the displacement of water and enhanced contact between patch and tissue surface. A compressive force of 3 N was selected for the remainder of this study given our ability to apply this compression *in vivo* and to ensure tight contact between patch and tissue during the curing process. Maximal adhesion was obtained when a 200- μ m-thick layer of HLAA was applied to the patch, and increasing the HLAA thickness did not affect adhesion (fig. S5C).

The versatility of the HLAA was explored for clinically available patch materials, such as bovine pericardium, porcine small intestine submucosa, and polyethylene terephthalate. After 5 s of curing, the measured pull-off adhesion forces against fresh epicardium were lower for these materials than for PGSU patches (Fig. 1F), but could be increased by curing for 30 s.

A major advantage of using an *in situ* curable adhesive is the possibility to activate the prepolymer with an external stimulus once correctly positioned. However, while navigating to the targeted site, adhesive washout can occur upon contact with blood or other fluids and potentially compromise its efficiency. This is especially relevant if adhesive-coated patches are exposed to blood flow. Thus, we evaluated the resistance of CA- and HLAA-coated patches in an experimental setup that mimicked dynamic exposure to blood before adhesion testing (fig. S6A). CA was immediately activated upon contact with blood, losing its ability to adhere to its intended substrate. In contrast, after exposure of the HLAA prepolymer to

flowing blood, no significant washout (fig. S6B) or change in adhesion strength (Fig. 1G) was observed.

The interaction between the HLAA and biological tissues

The interaction of the HLAA with biological tissue was evaluated *ex vivo* through Masson's trichrome (MT) staining and scanning electron microscopy (SEM) of the interface between the HLAA adhesive and cardiac tissue (Fig. 2, A and B). According to both techniques, the HLAA adhesive appears to infiltrate into the upper layer of the cardiac tissue. The SEM images revealed that upon fracture, the adhesive remains entangled within the collagen fibers. To confirm how the HLAA interacts and adheres to the tissue surface, we performed adhesion tests of the HLAA against functionalized coverslips with collagen. The HLAA showed strong adhesion against collagen-coated slides (Fig. 2C). Additionally, adhesion testing was performed against the adventitia of porcine carotid artery (Fig. 2D) given its similar chemical composition to the epicardium (that is, collagen), yet it exhibits a thicker layer of loose connective tissue that may favor interlocking. Despite the similar chemical composition, adhesion strength was higher for the adventitia than for the epicardium.

In vivo biocompatibility study

In vitro studies showed that the HLAA networks have a similar cytocompatibility profile to fibrin glue and improved when comparing with CA glue (fig. S7). To evaluate the *in vivo* biocompatibility and the adhesive potential of the HLAA under wet and dynamic conditions, we coated PGSU patches with the HLAA and attached them to the rat heart epicardium *in vivo* (Fig. 3A). For these studies, HLAA disinfection was based on the use of organic solvents during processing. HLAA- and CA-coated patches were attached to the epicardial surface of the rat heart (HLAA, $n = 8$; CA, $n = 7$). Patch repositioning was not possible for CA because it immediately cures upon contact with water. In contrast, owing to its “on-demand” polymerization and adhesion via UV light exposure, the HLAA-coated patches could be repositioned *in situ* at any time before activation.

After 7 days of implantation, 100% of the patches were attached in both groups ($n = 3$ per group). After 14 days of implantation (HLAA, $n = 5$; CA, $n = 4$), the degree of necrosis and inflammation was significantly less in the HLAA group compared to that in the CA group (Fig. 3, B and C). The nature of the inflammatory reaction was similar in the two groups. There were predominantly lymphocytes and macrophages surrounding the patches at 7 and 14 days. In contrast to CA, the infiltrate was reduced in size at 14 days for the HLAA. Cardiac function, determined by echocardiography, did not change over the course of the study for either group (fig. S8A).

Functional closure of transmural left ventricular wall defects

To further evaluate the adhesive potential of the HLAA, in particular its ability to achieve a hemostatic seal under dynamic conditions in the presence of blood and systemic pressures, we established a rat model of a transmural left ventricular (LV) wall defect (Fig. 3D). HLAA-coated patches were used to close LV wall defects *in vivo* in one animal group ($n = 19$) (movie S1), and this was compared to conventional suture-based closure in a control group ($n = 15$). Successful closure of the LV wall defect was achieved in 17 of 19 animals

that received the HLAA-coated patch, with 1 additional animal dying of bleeding complications on the fourth postoperative day. The three instances where the patch was not secured resulted in part from the inability to center the small (6-mm diameter) patch over the rapidly moving 2-mm defect. The heart rate of rats is six- to sevenfold higher than that of humans (23); thus, we do not anticipate that this will be a significant issue for clinical translation. Closure of the transmural wound with sutures was successful in 14 of 15 cases. The unsuccessful case was due to depressed LV function postoperatively.

Although echocardiographic analysis 28 days after LV puncture and closure revealed a reduced cardiac function in the area of the transmural LV wall defect, there was no significant difference in global cardiac function between the experimental groups (fig. S8B). Tissue scarring, with accumulation of organized collagen, was visible in both groups as a result of tissue damage to the tissue during defect creation (Fig. 3E).

Attachment of HLAA-coated patch to the septum of the beating heart

To demonstrate the ability of the HLAA to be used in the setting of beating heart intracardiac procedures, such as closure of ventricular septal defects, we developed a technique to attach a patch coated with the HLAA onto the interventricular septum of a pig's beating heart *in vivo*. We used a patch delivery system that consisted of a nitinol frame and a patch that could be released by withdrawing the nitinol wires holding the patch to the frame (Fig. 4A and fig. S9) (24). HLAA-coated patches (diameter, 10 mm) were then attached on the interventricular septum of the beating heart.

Successful attachment of the patch was achieved in all four animals tested with this device. Two animals were followed for 24 hours. No displacement of the patch could be detected by echocardiography before sacrifice ($n = 2$) (Fig. 4B). Epinephrine was administered in the other two animals 4 hours after patch placement, followed by sacrifice. Supra-normal heart rate and blood pressures were achieved: The peak heart rate averaged 186 beats per minute (range, 173 to 200 beats per minute), and the peak systolic blood pressure averaged 204 mmHg (range, 166 to 236 mmHg) ($n = 2$). The patch remained adherent to the tissue under this extremely dynamic environment (movie S2). Upon heart explantation, the patches were found to be affixed to the septum in all four animals, as confirmed by the stable patch position on the septum upon explantation (Fig. 4C). Histological analysis at 24 hours (Fig. 4D) revealed the formation of a fibrin capsule around the patch.

Closure of carotid artery defects with the HLAA

The use of the HLAA is not limited to the attachment of patches for defect closure. If the defect size allows, the HLAA polymer can be used on its own to create a leak-proof seal. To study this, we evaluated the *in vitro* burst pressure strength of the HLAA on explanted porcine carotid arteries. The defect (length, 3 to 4 mm) was covered with the viscous HLAA prepolymer followed by curing without application of pressure during curing (Fig. 5A). The average burst pressure was 203.5 ± 28.5 mmHg, which was greater than physiological systolic arterial pressure in humans (90 to 130 mmHg).

Defects (2-mm diameter) were then created in vivo in the carotid artery of four pigs. These defects were closed with the HLAA without a patch (Fig. 5B). All animals survived the procedure. Postoperative bleeding at 24 hours was not detected in any of the animals. Doppler imaging revealed blood flow 24 hours after sealing with HLAA (Fig. 5C). No thrombus formation was identified upon vessel explantation, and the adjacent endothelium was intact, as confirmed by H&E staining of the carotid arteries (Fig. 5D). We determined the thrombogenic potential of the HLAA and PGSU and compared to a thrombogenic material (glass). A lactate dehydrogenase assay was used to determine platelet attachment. HLAA exhibited 46% less platelet adhesion, and PGSU patches exhibited 65% less platelet adhesion compared to glass (Fig. 5E). These data are in line with previous reports for the hemocompatibility of PGS (25).

Discussion

We have developed an HLAA-based polymer that is nontoxic and bonds strongly to wet tissues and polymer surfaces even in the presence of blood. Owing to its optimized viscous and hydrophobic properties, the HLAA prepolymer exhibited minimal surface washout upon exposure to blood flow. Moreover, UV light activation permitted repositioning of the patches after delivery. Rapid curing helped to avoid exposure to high temperatures that can result from the UV light source. In contrast, there are no clinically available nontoxic surgical glues that can strongly bond tissues and that work on wet environments (2). Existing adhesives are associated with significant toxicity [for example, CA and bovine serum albumin (BSA)–glutaraldehyde] (26), low adhesive strength (for example, fibrin), or incompatibility with MIP. This incompatibility is due to the lack of control over the curing mechanism (that is, contact with water for CA, mixing two reactive components in situ for fibrin, and BSA–glutaraldehyde glues), which makes patch or device repositioning impossible. Often, physicians need to readjust the position of devices after delivery, especially in MIP with imaging guidance. Another challenge is the hydrophilicity of many adhesives, because they are easily displaced in the presence of flow. Other adhesives based on water-insoluble patch materials (for example, chitosan) are activated through the conversion of near-infrared radiation to thermal energy. However, the high temperatures generated (>60°C) produce tissue damage (27).

The soft, elastic nature of the HLAA (compression modulus of ~3 MPa and a tensile modulus of ~1 MPa) (21) and the patch material used (tensile modulus of ~5 MPa) combined with their low swelling in physiologic solutions (21, 22) is relevant for human soft tissue applications because it avoids tissue compression and friction that can induce damage (28). Cured HLAA exhibits mechanical properties similar to arteries and the gastrointestinal tract (29, 30). In contrast, CA exhibits a tensile modulus of 500 MPa, whereas fibrin gels have a compression modulus of 40 kPa and a limited ultimate strength that has led to leakage in human clinical applications (8, 31). The HLAA achieved its maximum adhesive strength at the specific degree of acrylation of 0.5 mol/mol glycerol, revealing the importance of optimizing the viscoelasticity of the material. The free hydroxyl groups in the polymeric network may also contribute to hydrogen bonding (32). Similar properties are relevant for other adhesives, for example, the performance of pressure-sensitive adhesives

results from the balance between fluidic properties, cohesion, and non-covalent bonding (33, 34).

The intimate contact between the HLAA and collagen fibers presented on the cardiac surface is a relevant characteristic of strong tissue adhesives (10, 35). We cannot exclude the contribution to adhesion of covalent bonding because of the radicals generated during the curing process (36), or hydrogen bonding owing to the presence of free hydroxyl groups in the polymeric network (32); however, the entanglement we observed through SEM imaging between the HLAA and collagen suggests that interlocking may play a major role.

The HLAA demonstrated excellent *in vivo* biocompatibility, which is crucial for an adhesive developed for internal use. In contrast, CA generated significant necrosis and tissue inflammation, as shown previously (8). The HLAA was evaluated in multiple functional *in vivo* models to demonstrate its effectiveness, biocompatibility, and applicability in cardiovascular surgery. The HLAA (21) and PGSU patch materials exhibited controllable *in vivo* degradation (22). Possible degradation products include glycerol, sebacic acid, products derived from the photoinitiator, as well as diamines resulting from the degradation of urethane groups in the patch material. Because the material's synthesis methods are solvent-based (dichloromethane and ethyl acetate are used for the PGSA synthesis), quantification of their residual levels will be required for human application. Nevertheless, the HLAA was bio-compatible, supporting long-term closure of the LV wall defect.

HLAA, by itself or in combination with a patch, created a hemostatic seal that was stable in dynamic environments and resisted systemic pressures. The HLAA could also be combined with multiple patch materials by adjusting the curing time, which increases its range of applicability. The ability of the HLAA prepolymer to maintain its adhesive capacity upon exposure to blood also opens new avenues in transcatheter interventional procedures and MIP. HLAA-coated patches could be delivered into the LV and attached to the interventricular septum through a minimal invasive technique and resisted extreme conditions characterized by supraphysiological heart rates and arterial pressures. Our experience with the HLAA-based patch attachment contrasts with reports using other adhesives, such as CA or BSA-glutaraldehyde glue (4), that require invasive open procedures, the use of sutures, and tissue drying before adhesive application. Longer-term experiments will be necessary to examine reendothelization in the carotid artery pig model and the overall performance of the adhesive patch in the intracardiac model. Although additional studies will be needed to confirm, patch dislodgment is unlikely after the establishment of a fibrous capsule that encases the patch (37).

The described HLAA should be useful to reduce the invasiveness of surgical procedures, reduce operative times, and consequently improve the outcome of cardiovascular procedures. This will be especially useful for pathologies that involve friable or specialized, delicate tissue. Moreover, the HLAA might offer a new practical and useful option for tissue repair or approximation in a wide variety of MIPs. Future work should focus on a better understanding of the adhesion mechanism for the HLAA to guide the design of next-generation formulations. Fine-tuning the material properties to enable delivery through small-bore needles, while ensuring minimum washout, will also be necessary. In addition, it

would be beneficial to explore the incorporation of bioactive molecules for controlled release applications. For translation into humans, additional safety and toxicity studies may be required. Here, we show that the HLAA has good hemostatic properties, even with large vessel defects. Therefore, the first step for human testing could be as hemostatic agent for suture line bleeding or small lacerations. For its use in vascular anastomosis, tissue-to-tissue approximation, or attaching devices or patches to the heart, additional long-term studies may be needed to demonstrate safety and efficacy.

Materials and Methods

Study design

The aim of this study was the development of a tissue adhesive for MIP. It was hypothesized that a hydrophobic and in situ activatable material would be advantageous because of minimum washout and controlled adhesion. In vitro work was performed to optimize the chemical composition and curing conditions of the HLAA material to maximize its adhesive and material performance compared to commonly used tissue adhesives. The application of the HLAA was explored in the context of cardiovascular surgery, because this is one of the most challenging fields in MIP due to the dynamic environment and presence of blood. The cardiac biocompatibility of the HLAA was assessed, and the results of this study were analyzed by a blinded pathologist. The ability of HLAA-coated patches and HLAA alone to provide a leak-proof seal was tested in small and large animals that were randomly selected for each experimental group. Finally, we showed that HLAA-coated patches can be deployed and attached under echo guidance, demonstrating its potential for MIP.

Synthesis of the HLAA

All chemicals were acquired from Sigma-Aldrich and used as received, unless specified otherwise. A PGS prepolymer was prepared through polycondensation of equimolar amounts of glycerol and sebacic acid (38). The formed prepolymer had an approximate weight average molecular weight of 5500 g/mol, determined through gel permeation chromatography (Viscotek TDA 305 with Agilent 1260 pump and autosampler, Malvern Instruments). The prepolymer was acrylated and purified as described (21). Briefly, PGS prepolymer was solubilized in dichloromethane in the presence of triethylamine and cooled to 0°C followed by the addition of acryloyl chloride. The mixture was allowed to react overnight. The material obtained was solubilized in ethyl acetate, filtered, and dried under vacuum at 40°C. The HLAA prepolymer was mixed with the photoinitiator Irgacure 2959 (0.2%, w/w) (39) and cured with a spot-curing UV light source (OmniCure S1000, Lumen Dynamics Group Inc.) equipped with a filter in the range of 320 to 390 nm. This wavelength range has been previously used to promote the encapsulation of cells in photocurable materials, with minimal cytotoxicity (40). The curing time was 5 s, and the light intensity was 0.38 W/cm² unless otherwise specified. Chemical and mechanical characterization of the resulting polymer is described in the Supplementary Materials and Methods.

PGSU patch synthesis

A PGSU patch was synthesized as described in the Supplementary Materials (22).

Adhesion testing

Pull-off adhesion testing (at 90°) was performed on an ADMET eXpert 7601 universal tester with fresh porcine epicardial tissue. The tissue was kept in phosphate-buffered saline to assure that it remained wet during testing. Unless specified, a PGSU patch was used for testing and was about 200 µm thick and 6 mm in diameter. A thin layer of the HLAA, with a thickness of about 200 µm, was applied to the patch material before adhesion testing. During the curing process, a compressive force of -3 N was applied to the HLAA-coated patch with a nonadhesive material (borosilicate glass rod 9 mm in height) connected to the UV light guide (Lumen Dynamics Group Inc.; light intensity, 0.38 W/cm²) with standard adhesive tape around both the glass rod and the light guide. The interposition of the borosilicate glass rod facilitates the release of the curing system from the patch without disturbing the patch/adhesive-tissue interface. The pull-off procedure involved the controlled application of a preload (-1 N) to the adherent PGSU patch followed by grip separation at a rate of 8 mm/min, causing uniform patch detachment from the tissue surface. Adhesion force was recorded as the maximum force observed before adhesive failure, when a sharp decrease in the measured stress was observed.

The adhesive forces of fibrin (TissuSeal, $n = 4$) and CA (Dermabond, $n = 3$) coatings on PGSU 1:0.5 patches were measured. The effect of curing time (1, 5, and 30 s; $n = 4$ per condition) on the adhesive strength of the HLAA was tested. Adhesion of different patch materials used in cardiovascular surgery (Supple Peri-Guard, CorMatrix, and Dacron; $n > 4$ per patch material) was also tested. To examine the ability of adhesives to resist washout and cure after exposure to flowing blood, PGSU patches coated with HLAA prepolymer or CA were exposed to heparinized blood for 5 min in an incubated shaker at 500 rpm and 37°C ($n = 3$) followed by pull-off adhesion testing. The adhesive strength of PGSU patches coated with uncured HLAA or CA against wet epicardial tissue was used as a control.

Evaluation of the interaction of the HLAA with biological tissues

The adhesion of HLAA-coated PGSU patches on functionalized glass collagen (BD Biosciences) was examined through pull-off testing as described above. Unmodified glass surfaces served as a control. In addition, HLAA-coated patches were attached to fresh pig epicardial tissue, and MT staining was performed to characterize the tissue-material interface.

We performed freeze fracture of heart tissue with attached HLAA-coated PGSU patches to further examine the interaction. Samples were prepared as described in the “Adhesion testing” section. The prepared samples were fixed in Karnovsky fixative [0.1 M phosphate buffer, 2% paraformaldehyde (PFA), 2.5% glutaraldehyde, final pH 7.2] overnight, dehydrated with ethanol, and critical-dried before fracture. The dried samples were manually fractured and sputter-coated with platinum for SEM (AMRAY AMR-1000).

Animals

Male Wistar rats (300 to 350 g, Charles River Laboratories International) and Yorkshire pigs (70 to 80 kg for the intracardiac study and 40 to 50 kg for the vascular study, Parsons EM & Sons Inc.) were used. The in vivo studies were conducted in accordance with the *Guide for*

the Care and Use of Laboratory Animals. Euthanasia of rats and pigs was performed with CO₂ and Fatal-Plus, respectively. The animal protocols were reviewed and approved by the Animal Care Committee at Boston Children's Hospital.

Functional closure of LV wall defects with HLAA-coated patches in a rat model

Preoperative echocardiography, anesthesia, and surgical preparation were performed as described in the Supplementary Materials. After exposure of the LV, a transmural LV wall defect was created with a 2-mm puncher (Integra Miltex). Before defect creation, a purse-string suture was applied at the desired position to prevent bleeding. The defects were closed with an HLAA-coated PGSU patch (diameter, 6 mm). Subsequently, the purse string suture was removed. In some cases, an immediate hemostatic seal was not achieved because the patch was not exactly centered over the defect and bleeding at the edges of the patch was observed. To achieve a complete seal, additional glue was applied to the edges of the patch with a pipette tip and then cured for 5 s (movie S1). A separate group of animals underwent purse-string suture closure of the LV wall defect without the HLAA. Postoperative echocardiography and euthanasia were performed after 7, 28, 90, and 180 days (HLAA: $n = 2$ with initial unsuccessful closure, $n = 5$ for 7 and 28 days, $n = 4$ for 90 days, and $n = 3$ for 180 days; sutures: $n = 4$ for 7, 28, and 90 days, $n = 3$ for 180 days). Hearts were explanted and fixed in 4% PFA, and H&E and MT staining were performed.

Intracardiac delivery and attachment of HLAA-coated patches in a pig model

Anesthesia and surgical preparation were performed as described previously. Briefly, a left thoracotomy in the fifth or sixth intercostal space was performed to expose the heart. The entire procedure was performed without CPB. Two-dimensional (2D) and 3D epicardial echocardiography with an X4 matrix probe on a SONOS 7500 system (Philips Medical Systems) was used for imaging inside the beating heart. HLAA-coated patches (diameter, 10 mm) were attached to the ventricular septum with a specifically developed technique.

Two animals were monitored for 4 hours after the procedure. An epinephrine bolus was then administered, and patch position was monitored via echocardiography to evaluate the effect of elevated blood pressure and heart rate. After this, the animals were euthanized for histological analysis. Another two animals were monitored for 24 hours and then euthanized. The hearts were explanted and fixed with 4% PFA, and H&E staining was performed.

Closure of carotid artery defects with the HLAA in vitro and in vivo

In vitro burst pressure testing was performed on freshly explanted swine carotid arteries ($n = 3$). Briefly, one end the vessel was connected to a syringe driver and a pressure transducer (Honeywell T&M), and the other end was closed with a custom-made plug. A 3- to 4-mm longitudinal incision was made in the vessel wall. The incision and surrounding vessel wall (covering an area of ~ 1 cm²) were coated with the HLAA and cured for 20 s without pressure application. Saline was infused at 60 ml/min, and the burst pressure was recorded (eXpert 3600 Biaxial, ADMET).

For the in vivo study, animals ($n = 4$ pigs) were anesthetized as described above. Ultrasound with color Doppler of the left carotid artery was performed preoperatively to confirm normal blood flow. The left neck was then incised, and the carotid artery was exposed and controlled proximally and distally with vascular clamps. A 2-mm longitudinal incision was made in the vessel. The incision was closed with the HLAA as described above. The vascular clamps were released, and the carotid artery was inspected for up to 10 min to detect bleeding. After 24 hours of monitoring, ultrasound with color Doppler was performed to evaluate blood flow. Subsequently, the animals were euthanized, and the carotid artery was fixed with 4% PFA. H&E staining was performed on cross sections of the center and edges of the defect.

Statistical analysis

Data are expressed as means \pm SD. Graphs were created by the GraphPad Prism software. Statistical analysis was performed with SigmaStat software. For in vitro adhesion tests, three independent experiments were performed and the mean value was determined. The Kolmogorov-Smirnov normality test was used for assessing normality. In addition, equal variance was evaluated with the f test. One-way ANOVA with post hoc Tukey testing was used to examine statistical differences between multiple groups. Unpaired t test was used to examine statistical differences between two independent groups. For the data set obtained in the experiment aiming to evaluate the adhesion of different HLAA-coated patch materials exposed for 5 or 30 s to UV light, equal variance could not be confirmed. Therefore, the Mann-Whitney rank sum test for independent groups was performed. Results were considered significant when a P value of < 0.05 was obtained.

Supplementary Material

Refer to Web version on PubMed Central for supplementary material.

Acknowledgments

We thank P. Hammer for critical comments throughout the project; K. Mullen, A. Nedder, and H. Yamauchi for assistance with the in vivo experiments; O. Miranda for assistance with the NMR; W. Fowle for assistance with SEM; and ADMET Inc. for providing an eXpert 7601 mechanical tester that was instrumental for this work.

Funding: This work was supported by the Center for Integration of Medicine and Innovative Technology grant 11-315 and W81XWH-09-2-0001, the Technology Research Program grant of Boston Children's Hospital, and NIH grant HL73647 to P.J.d.N. This work was also supported by the NIH grants GM086433 (to J.M.K.) and DE013023 (to R.L.). M.J.P. acknowledges the Portuguese Foundation for Science and Technology (fellowship SFR/BD/43013/2008) and the MIT-Portugal program (bioengineering focus area). N.L. acknowledges the German Research Foundation (DFG) for financial support (LA 2865/1-1).

References and Notes

1. Spotnitz WD. Hemostats, sealants, and adhesives: A practical guide for the surgeon. *Am Surg.* 2012; 78:1305–1321. [PubMed: 23265118]
2. Dolgin E. The sticking point. *Nat Med.* 2013; 19:124–125. [PubMed: 23389599]
3. Chang EI, Galvez MG, Glotzbach JP, Hamou CD, El-ftesi S, Rappleye CT, Sommer KM, Rajadas J, Abilez OJ, Fuller GG, Longaker MT, Gurtner GC. Vascular anastomosis using controlled phase transitions in poloxamer gels. *Nat Med.* 2011; 17:1147–1152. [PubMed: 21873986]

4. Cheema FH, Younus MJ, Roberts HG Jr. Repairing the posterior postinfarction ventricular septal defect: A left ventricular approach with a sealant reinforced multipatch technique. *Semin Thorac Cardiovasc Surg.* 2012; 24:63–66. [PubMed: 22643664]
5. Predescu D, Chaturvedi RR, Friedberg MK, Benson LN, Ozawa A, Lee KJ. Complete heart block associated with device closure of perimembranous ventricular septal defects. *J Thorac Cardiovasc Surg.* 2008; 136:1223–1228. [PubMed: 19026807]
6. Crawford GB, Brindis RG, Krucoff MW, Mansalis BP, Carroll JD. Percutaneous atrial Septal Occluder devices and cardiac erosion: A review of the literature. *Catheter Cardiovasc Interv.* 2012; 80:157–167. [PubMed: 22552868]
7. Elefteriades JA. How I do it: Utilization of high-pressure sealants in aortic reconstruction. *J Cardiothorac Surg.* 2009; 4:27. [PubMed: 19558685]
8. Mizrahi B, Stefanescu CF, Yang C, Lawlor MW, Ko D, Langer R, Kohane DS. Elasticity and safety of alkoxyethyl cyanoacrylate tissue adhesives. *Acta Biomater.* 2011; 7:3150–3157. [PubMed: 21569875]
9. Duarte AP, Coelho JF, Bordado JC, Cidade MT, Gil MH. Surgical adhesives: Systematic review of the main types and development forecast. *Prog Polym Sci.* 2012; 37:1031–1050.
10. Artzi N, Shazly T, Baker A, Bon A, Edelman E. Aldehyde-amine chemistry enables modulated biosealants with tissue-specific adhesion. *Adv Mater.* 2009; 21:3399–3403. [PubMed: 20882504]
11. Smith AM, Robinson TM, Salt MD, Hamilton KS, Silvia BE, Blasiak R. Robust cross-links in molluscan adhesive gels: Testing for contributions from hydrophobic and electrostatic interactions. *Comp Biochem Physiol B Biochem Mol Biol.* 2009; 152:110–117. [PubMed: 18952190]
12. Shao H, Stewart RJ. Biomimetic underwater adhesives with environmentally triggered setting mechanisms. *Adv Mater.* 2010; 22:729–733. [PubMed: 20217779]
13. Federle W, Riehle M, Curtis ASG, Full RJ. An integrative study of insect adhesion: Mechanics and wet adhesion of pretarsal pads in ants. *Integr Comp Biol.* 2002; 42:1100–1106. [PubMed: 21680393]
14. Matsuda M, Inoue M, Taguchi T. Adhesive properties and biocompatibility of tissue adhesives composed of various hydrophobically modified gelatins and disuccinimidyl tartrate. *J Bioact Compat Polym.* 2012; 27:481–498.
15. Matteini P, Ratto F, Rossi F, Pini R. Emerging concepts of laser-activated nanoparticles for tissue bonding. *J Biomed Opt.* 2012; 17:010701. [PubMed: 22352632]
16. Lauto A, Foster LJ, Ferris L, Avolio A, Zwaneveld N, Poole-Warren LA. Albumin–genipin solder for laser tissue repair. *Lasers Surg Med.* 2004; 35:140–145. [PubMed: 15334618]
17. O'Neill AC, Winograd JM, Zeballos JL, Johnson TS, Randolph MA, Bujold KE, Kochevar IE, Redmond RW. Microvascular anastomosis using a photochemical tissue bonding technique. *Lasers Surg Med.* 2007; 39:716–722. [PubMed: 17960755]
18. Hoogbeem JE, Ranger WR, Leibold WC. Pneumostasis of experimental air leaks with a new photopolymerized synthetic tissue sealant—Discussion. *Am Surg.* 1997; 63:795.
19. Elvin CM, Brownlee AG, Huson MG, Tebb TA, Kim M, Lyons RE, Vuocolo T, Liyou NE, Hughes TC, Ramshaw JA, Werkmeister JA. The development of photochemically cross-linked native fibrinogen as a rapidly formed and mechanically strong surgical tissue sealant. *Biomaterials.* 2009; 30:2059–2065. [PubMed: 19147224]
20. Spencer HT, Hsu JT, McDonald DR, Karlin LI. Intraoperative anaphylaxis to gelatin in topical hemostatic agents during anterior spinal fusion: A case report. *Spine J.* 2012; 12:e1–e6. [PubMed: 23021035]
21. Nijst CL, Bruggeman JP, Karp JM, Ferreira L, Zumbuehl A, Bettinger CJ, Langer R. Synthesis and characterization of photocurable elastomers from poly(glycerol-co-sebacate). *Biomacromolecules.* 2007; 8:3067–3073. [PubMed: 17725319]
22. Pereira MJ, Ouyang B, Sundback CA, Lang N, Friehs I, Mureli S, Pomerantseva I, McFadden J, Mochel MC, Mwizerwa O, Del Nido P, Sarkar D, Masiakos PT, Langer R, Ferreira LS, Karp JM. A highly tunable biocompatible and multifunctional biodegradable elastomer. *Adv Mater.* 2013; 25:1209–1215. [PubMed: 23239051]
23. Tan I, Butlin M, Liu YY, Ng K, Avolio AP. Heart rate dependence of aortic pulse wave velocity at different arterial pressures in rats. *Hypertension.* 2012; 60:528–533. [PubMed: 22585952]

24. Kozlik-Feldmann R, Lang N, Aumann R, Lehner A, Rassouljian D, Sodian R, Schmitz C, Hinterseer M, Hinkel R, Thein E, Freudenthal F, Vasilyev NV, del Nido PJ, Netz H. Patch closure of muscular ventricular septal defects with a new hybrid therapy in a pig model. *J Am Coll Cardiol.* 2008; 51:1597–1603. [PubMed: 18420104]
25. Motlagh D, Yang J, Lui KY, Webb AR, Ameer GA. Hemocompatibility evaluation of poly(glycerol-sebacate) in vitro for vascular tissue engineering. *Biomaterials.* 2006; 27:4315–4324. [PubMed: 16675010]
26. Alameddine A, Alimov VK, Rousou JA, Freeman J. Aorto-pulmonary artery disruption following acute type-A aortic dissection repair with the use of BioGlue®. *J Card Surg.* 2012; 27:371–373. [PubMed: 22500618]
27. Lauto A, Hook J, Doran M, Camacho F, Poole-Warren LA, Avolio A, Foster LJ. Chitosan adhesive for laser tissue repair: In vitro characterization. *Lasers Surg Med.* 2005; 36:193–201. [PubMed: 15704155]
28. Lee G, Lee C, Bynevelt M. DuraSeal-hematoma: Concealed hematoma causing spinal cord compression. *Spine.* 2010; 35:E1522–E1524. [PubMed: 21102284]
29. Serrano MC, Chung EJ, Ameer GA. Advances and applications of biodegradable elastomers in regenerative medicine. *Adv Funct Mat.* 2010; 20:192–208.
30. Egorov VI, Schastlivtsev IV, Prut EV, Baranov AO, Turusov RA. Mechanical properties of the human gastrointestinal tract. *J Biomech.* 2002; 35:1417–1425. [PubMed: 12231288]
31. Rowe SL, Lee S, Stegemann JP. Influence of thrombin concentration on the mechanical and morphological properties of cell-seeded fibrin hydrogels. *Acta Biomater.* 2007; 3:59–67. [PubMed: 17085089]
32. Smart JD. The basics and underlying mechanisms of mucoadhesion. *Adv. Drug Deliv Rev.* 2005; 57:1556–1568.
33. Feldstein MM, Siegel RA. Molecular and nanoscale factors governing pressure-sensitive adhesion strength of viscoelastic polymers. *J Polym Sci B Polym Phys.* 2012; 50:739–772.
34. Chung H, Glass P, Pothen J, Sitti M, Washburn N. Enhanced adhesion of dopamine methacrylamide elastomers via viscoelasticity tuning. *Biomacromolecules.* 2011; 12:342–347. [PubMed: 21182292]
35. Mahdavi A, Ferreira L, Sundback C, Nichol JW, Chan EP, Carter DJ, Bettinger CJ, Patanavanich S, Chignozha L, Ben-Joseph E, Galakatos A, Pryor H, Pomerantseva I, Masiakos PT, Faquin W, Zumbuehl A, Hong S, Borenstein J, Vacanti J, Langer R, Karp JM. A biodegradable and biocompatible gecko-inspired tissue adhesive. *Proc Natl Acad Sci USA.* 2008; 105:2307–2312. [PubMed: 18287082]
36. Yao M, Yaroslavsky A, Henry FP, Redmond RW, Kochevar IE. Phototoxicity is not associated with photochemical tissue bonding of skin. *Lasers Surg Med.* 2010; 42:123–131. [PubMed: 20166159]
37. Sideris EB. Advances in transcatheter patch occlusion of heart defects. *J Interv Cardiol.* 2003; 16:419–424. [PubMed: 14603801]
38. Wang Y, Ameer GA, Sheppard BJ, Langer R. A tough biodegradable elastomer. *Nat Biotechnol.* 2002; 20:602–606. [PubMed: 12042865]
39. Williams C, Malik A, Kim T, Manson P, Elisseeff J. Variable cytocompatibility of six cell lines with photoinitiators used for polymerizing hydrogels and cell encapsulation. *Biomaterials.* 2005; 26:1211–1218. [PubMed: 15475050]
40. Khetan S, Guvendiren M, Legant WR, Cohen DM, Chen CS, Burdick JA. Degradation-mediated cellular traction directs stem cell fate in covalently crosslinked three-dimensional hydrogels. *Nat Mater.* 2013; 12:458–465. [PubMed: 23524375]

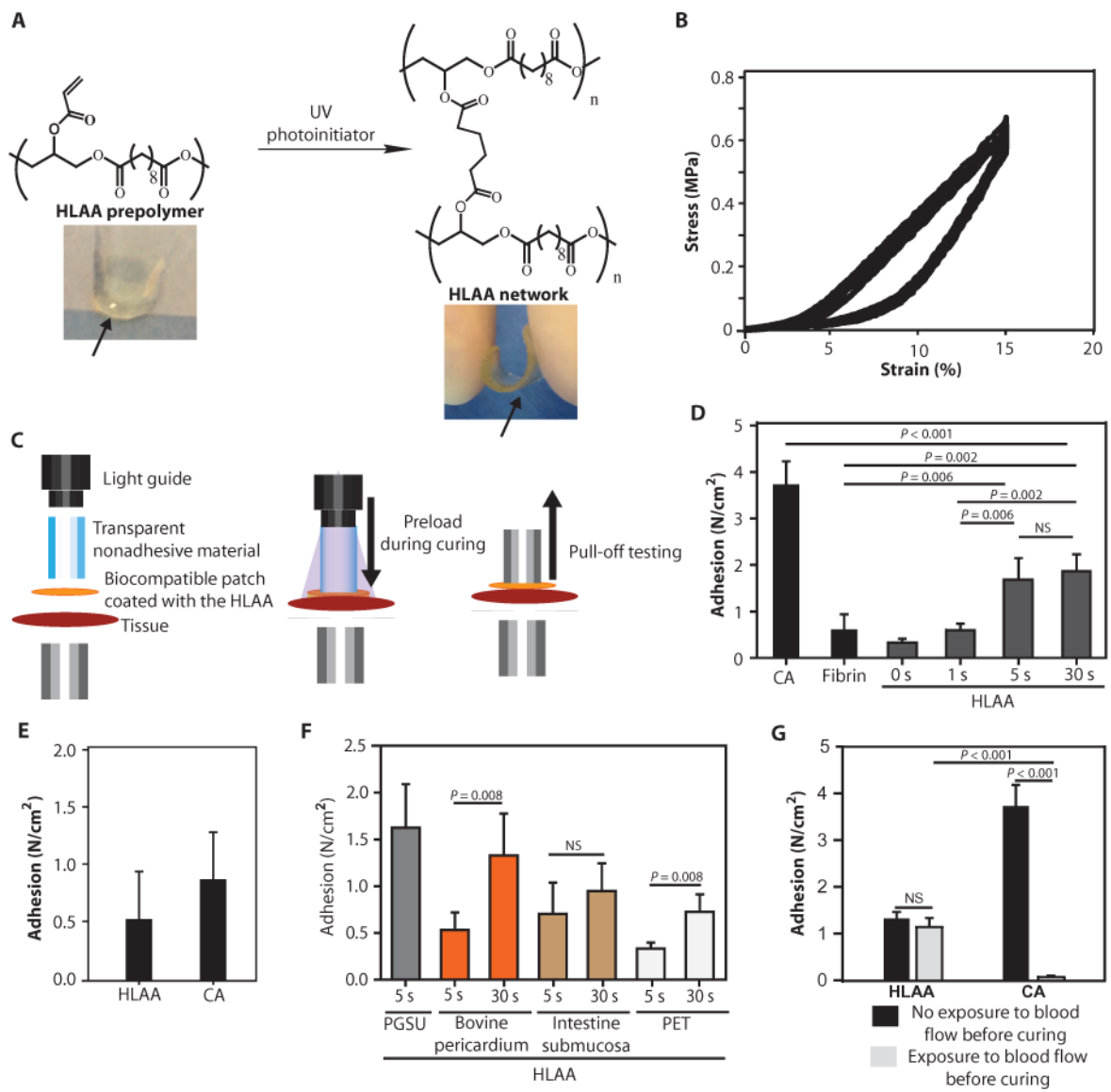


Fig. 1. Elastic and adhesive properties of the HLAA on wet biological tissues

(A) Chemical structure of the HLAA before and after exposure to UV light. (B) HLAA properties under cyclical loading. (C) Pull-off method for testing adhesive strength of the HLAA. First, the tissue was glued onto a flat metal substrate, and the patch coated with the HLAA was pressed against the tissue using a transparent nonadhesive material and the UV light guide with a preload of -3 N. UV light was applied to activate the HLAA and the transparent nonadhesive material, and the UV light guide was then removed. A second flat metal substrate was glued to the patch for pull-off testing. (D) Pull-off adhesion strength of fibrin sealant, CA, and HLAA exposed to UV light for different periods of time (0, 1, 5, or 30 s) against epicardial tissue (fibrin: $n = 4$, CA: $n = 3$, HLAA: $n = 4$). PGSU patch material was used for all the experiments. P values were determined by one-way analysis of variance (ANOVA) with the Tukey post hoc test. (E) In vivo adhesion strength of HLAA- and CA-coated patches after 2 days of implantation. Strengths were determined using a pull-off

procedure on explanted rat epicardium ($n = 3$). **(F)** Adhesion strength using PGSU and clinically used patch materials against fresh cardiac tissue ($n = 5$). P values were determined by Mann-Whitney rank sum test. PET, polyethylene terephthalate. **(G)** HLAA and CA adhesion with or without exposure to blood before contact with cardiac tissue ($n = 3$). P values were determined by one-way ANOVA with Tukey post hoc testing. Data in **(D)** to **(G)** are means \pm SD. NS, not significant.

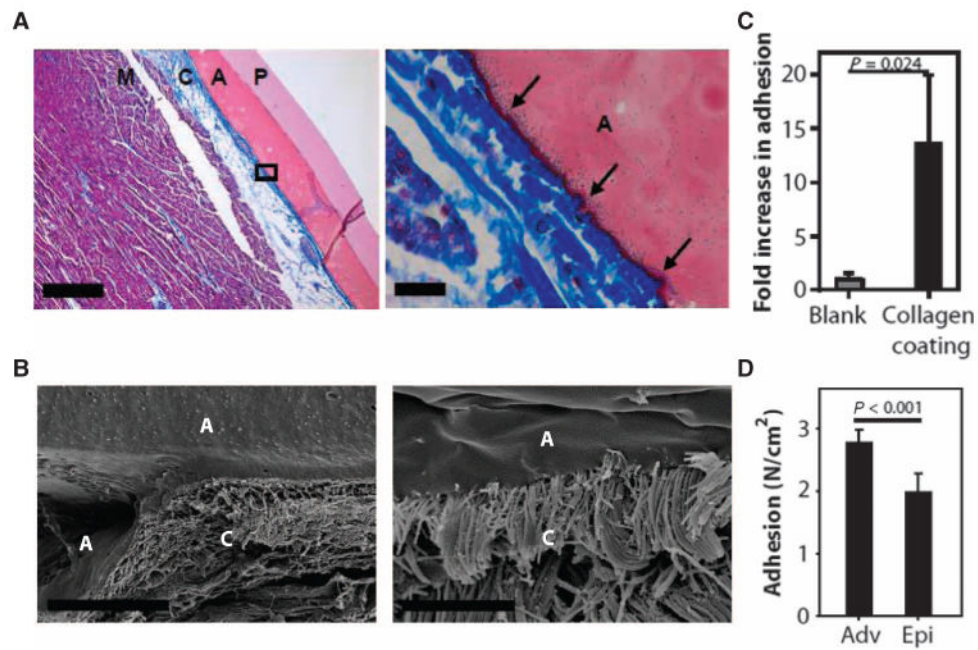


Fig. 2. Interaction between the HLAA and collagen substrates

(A) The HLAA-coated patch was applied ex vivo to porcine epicardium, and the interface was examined using MT staining. M, myocardium; C, collagen; A, HLAA; P, PGSU patch. The HLAA appeared to entangle with epicardium collagen fibers (arrows). Scale bars, 500 μ m (left) and 20 μ m (right). (B) Freeze-fractured HLAA-tissue interface observed with SEM for endocardium (left) and epicardium (right) tissues. Scale bars, 30 and 2 μ m, respectively. (C) Controlled adhesion tests were performed on glass slides coated with collagen type I. Data are means \pm SD ($n = 3$). (D) HLAA pull-off adhesion strength against the adventitia of pig carotid artery and epicardium tissue. Data are means \pm SD ($n = 5$). *P* values in (C) and (D) were determined by unpaired *t* test.

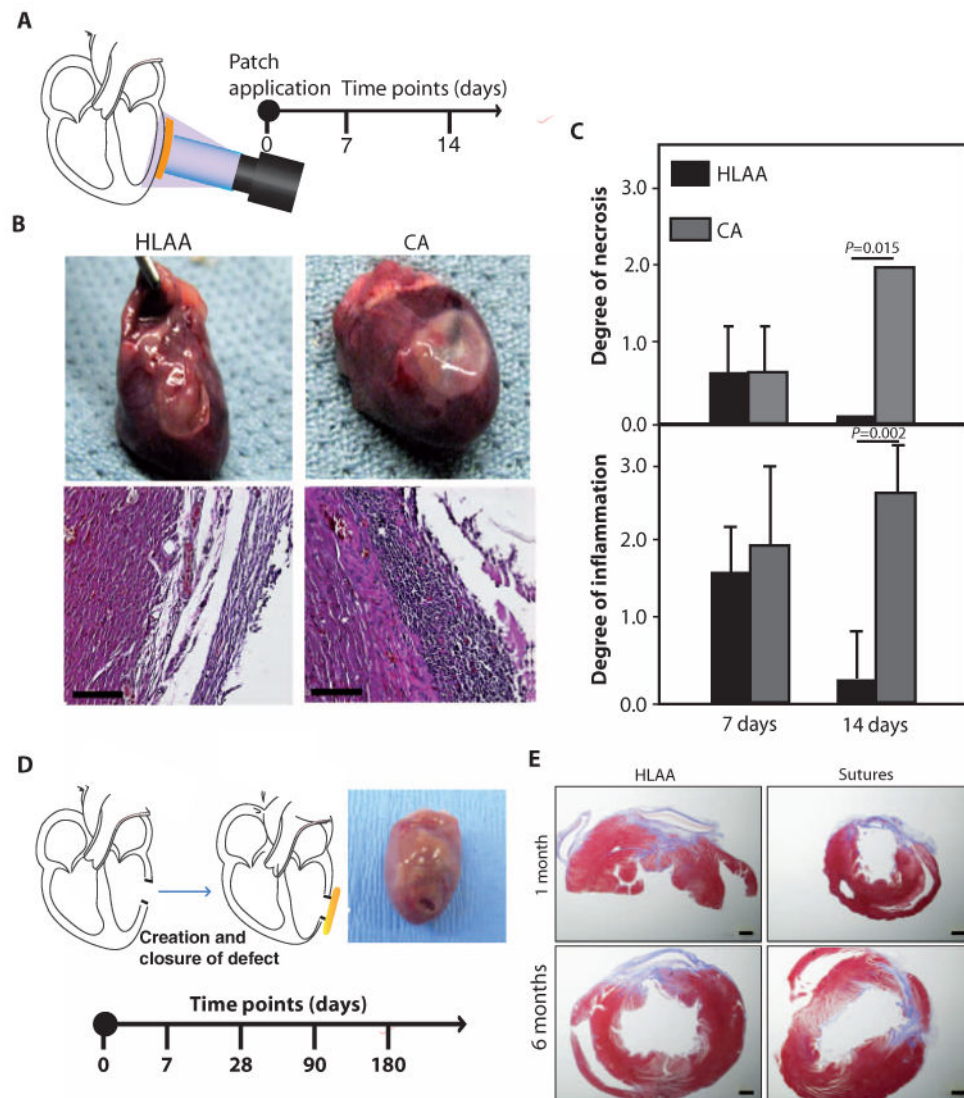


Fig. 3. In vivo biocompatibility and adhesive strength testing of HLAA- and CA-coated elastomeric patches

(A) Experimental methodology and time points selected to evaluate the biocompatibility of the HLAA. CA was used as the control. (B) Explanted hearts 14 days after implantation and corresponding hematoxylin and eosin (H&E) staining of the cardiac tissue in contact with the adhesives. A thicker layer of inflammatory cells was observed for CA, as indicated by arrowheads. Scale bars, 500 μ m. (C) The degree of tissue necrosis and inflammation for the HLAA and CA (0, negligible; 1, reduced; 2, moderate; 3, severe) was scored by a blinded pathologist. Data are means \pm SD ($n = 3$). P values were determined by one-way ANOVA with Tukey post hoc testing. (D) Experimental methodology and selected time points for closure of LV free wall cardiac defects in the rat. A 2-mm defect was created and closed with a patch (diameter, 6 mm) coated with the HLAA. Closure of the defect with sutures was used as a control. (E) Representative H&E- and MT-stained sections at 1 and 6 months after defect closure for the suture and HLAA groups ($n = 3$). Scale bars, 1 mm.

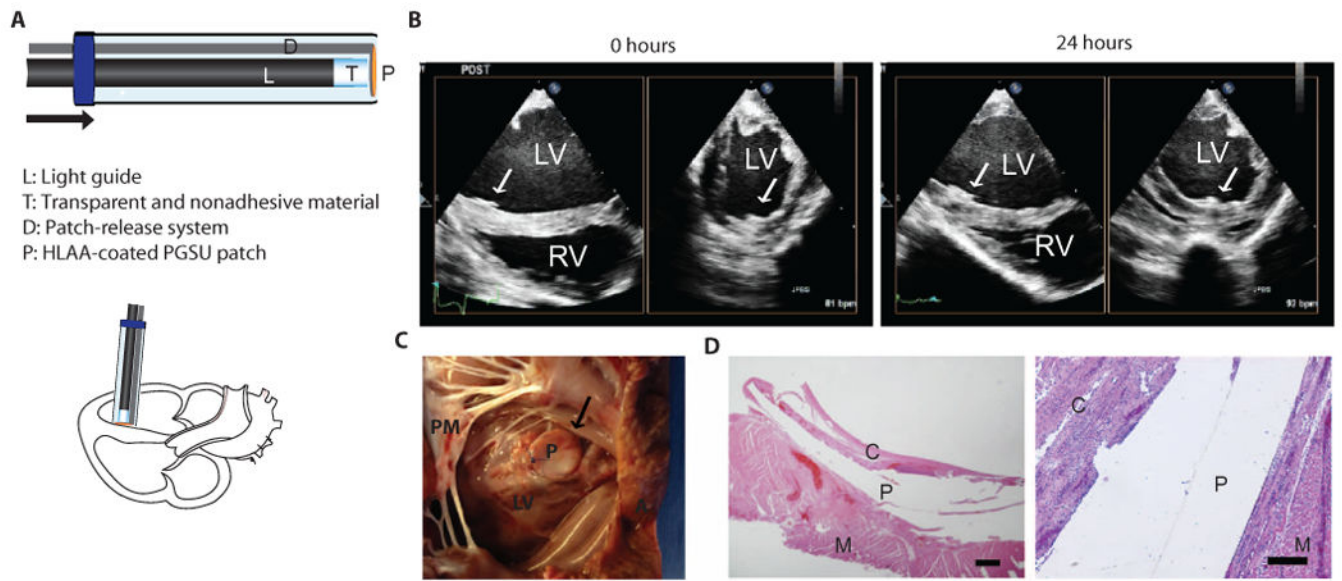


Fig. 4. HLA-coated patches attach to beating hearts in vivo in a large animal model
 (A) Device and technique for minimally invasive patch delivery and attachment to the pig heart through a single LV incision. (B) Echocardiographic evaluation of patch location 0 hours ($n = 4$) and 24 hours ($n = 2$) after patch attachment. LV, left ventricle; RV, right ventricle. (C) Location of the deployed patch 24 hours after initial application (A, apex; P, patch; PM, papillary muscles; LV, left ventricle). (D) H&E stain of the tissue surrounding the patch material after 4 hours ($n = 2$) and 24 hours ($n = 2$) of implantation. M, myocardium; P, patch; C, capsule. Scale bars, 1 mm (left) and 200 μm (right).

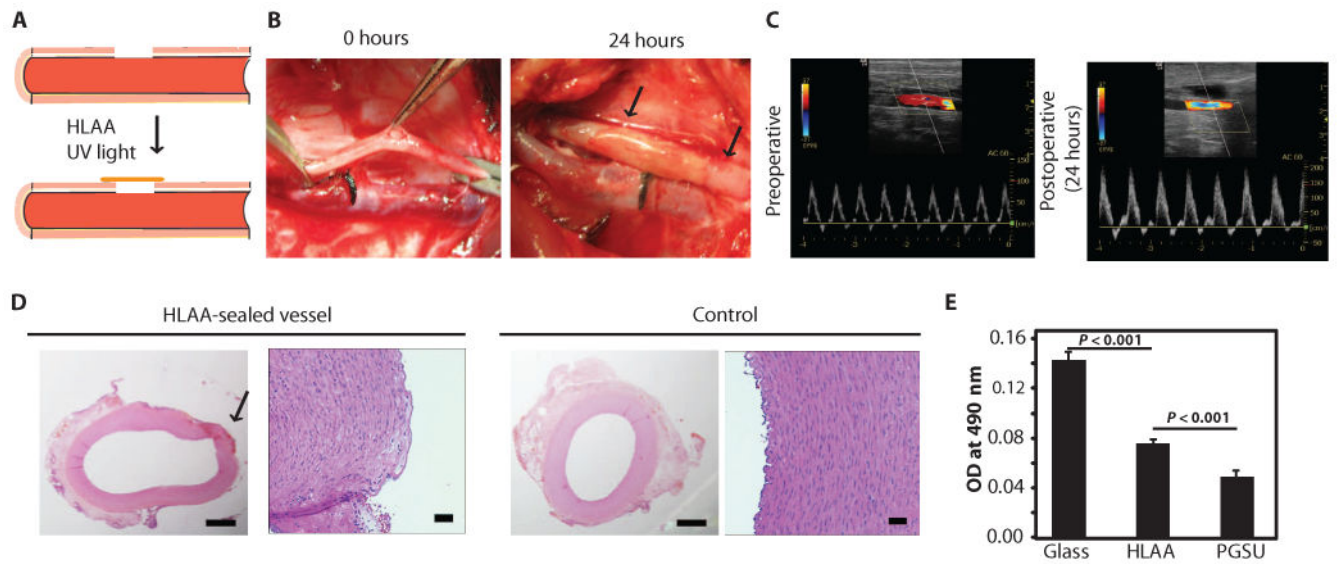


Fig. 5. HLAA alone can close vascular defects

(A) A 2-mm incision on ex vivo porcine carotid arteries was closed with the HLAA, without a patch. (B) Carotid artery after defect creation and 24 hours after closure with the HLAA. (C) Doppler images demonstrating vessel flow before defect creation and 24 hours after closure. (D) H&E-stained sections from the HLAA-treated vessels (left) and a noninjured carotid artery (right). Arrow points to the defect created. Images are representative of $n = 4$ animals. Scale bars, 1 mm (left) and 50 μm (right). (E) Thrombogenic response of HLAA. The lactate dehydrogenase colorimetric signal was determined after incubating glass, HLAA, and PGSU with porcine blood for 1 hour. Data are means \pm SD ($n = 5$). *P* values were determined by one-way ANOVA with Tukey post hoc test.